Linear tuning of charge carriers in graphene by organic molecules and charge-transfer complexes

J. T. Sun,[1] Y. H. Lu,[2] W. Chen,[1,2] Y. P. Feng,[2,*] and A. T. S. Wee[2,†]
[1]*Department of Chemistry, National University of Singapore, 3 Science Drive 3, Singapore 117543, Singapore*
[2]*Department of Physics, National University of Singapore, 2 Science Drive 3, Singapore 117542, Singapore*
(Received 11 November 2009; revised manuscript received 10 February 2010; published 1 April 2010)

The electronic interactions of several organic donor/acceptor molecules or combination of these molecules (hereafter known as "charge-transfer complexes") with graphene have been investigated by first-principles calculations and photoemission spectroscopy experiments. It is found that the doping behavior of graphene can be controlled by the ratio of donor and acceptor molecules in the form of their charge-transfer complexes. The interfacial electronic structure of molecules adsorbed on graphene is dominated by the charge-transfer mechanism. The changes in work function of graphene modified by organic molecules are discussed in comparison with experiments and they are in good agreement with experimental data. Our results show that functionalization of graphene by acceptor/donor molecules and their charge-transfer complexes is an efficient way to control the doping behavior of graphene.

DOI: 10.1103/PhysRevB.81.155403 PACS number(s): 73.22.−f, 31.10.+z, 68.43.−h, 31.15.E−

I. INTRODUCTION

Graphene, a single layer of graphite, was predicted to have many interesting and potentially useful properties such as high electron mobility, quantization of the conductivity, and a zero-energy anomaly in the quantum-Hall effect.[1–3] These intriguing behaviors are attributed to the peculiar electronic structure of graphene. The conduction and valence bands of graphene touch each other at the K points in the Brillouin zone, resulting in a zero-energy gap and vanishing density of states at the Fermi level.[4,5] The energy dispersion in reciprocal space is essentially linear within ± 1 eV with respect to the Dirac point. Consequently, graphene is believed to be one of the most promising materials for future electronic devices since conventional Si-based electronics have encountered fundamental limitations when the spatial scale reaches below 10 nm.

Since graphene has a two-dimensional structure with a single-atom thickness, it can be easily integrated into electronic circuits with source and drain leads.[6] However, as a prerequisite to the development of graphene-based electronic devices, the ability to control the type and concentration of its charge carriers is crucial. The electronic structure of graphene can be modified by external fields,[6,7] chemical adsorption,[8–12] strain,[13] intercalation,[14] periodic potential,[15,16] or by controlling the stacking symmetry of graphene bilayers.[17] Among these approaches, doping graphene by external chemical species is an effective way of controlling the charge-carrier type and concentration and has received much attention.[18–22] A variety of doping behaviors can be achieved upon the adsorption of graphene on metal substrates due to the different interfacial interactions between them.[20–22] Epitaxially grown graphene on wide-band semiconductor 6H-SiC(0001) can also be tuned into hole doping by atomic adsorption of bismuth, antimony, and gold.[23] Recently, Chen *et al.*[24] has demonstrated that the p-type doped epitaxial graphene can be obtained by adsorption of the strong electron-acceptor tetrafluorotetracyanoquinodimethane (F4-TCNQ). This technique gives a simple and effective method to dope graphene for future nanoelectronic applications. In this work, we have shown, by first-principles electronic-structure calculations, that the doping behavior of graphene can be controlled by coadsorption of charge-transfer complexes (CTC) consisting of a mix of donor and acceptor molecules. We investigate the interfacial electronic structures between graphene and donor/acceptor molecules, focusing on the changes in the electronic structure of graphene by the adsorbed molecules or CTC. The selected molecules include tetrathiofulvalene (TTF), TCNQ, and F4-TCNQ, which are electronic materials with potential applications for future organic eletronics.[25] In particular, F4-TCNQ has been successfully used as effective p-type dopant for organic semiconductors, carbon nanotubes, graphene, and diamond. Their combinations (CTC) have been investigated systematically in crystalline form or on metal surfaces.[26,27] Here TTF is an electron-donating molecule while TCNQ and F4-TCNQ are electron-accepting molecules with different electron affinities. CTC of desired electron-donating/accepting characteristics can be obtained by using a mix of these molecules in appropriate ratios. Density-functional theory (DFT) calculations show that the type and concentration of charge carriers in graphene can be linearly tuned by the molecular ratio in the CTC. Results of the calculations are compared to that from photoemission spectroscopy (PES) experiments. Compared to adsorptions of the same molecules on metal surfaces,[28,29] interactions between graphene and the acceptor molecules (TCNQ or F4-TCNQ), in single and CTC forms, are much stronger, due to the π-π interaction between TCNQ/F4-TCNQ and graphene.

II. METHODOLOGY

First-principles calculations were carried out using the VASP code.[30–33] The most important parameter is possibly the exchange-correlation functional. It is well known that the local density approximation (LDA) (Ref. 34) functional performs better in describing the interaction between molecules and graphene than the generalized gradient approximation

(GGA) functional. GGA overestimates the separation between graphene and the molecules while LDA yields acceptable separations. The electron-ion interaction was approximated by the projector augmented wave potential.[35,36] The electron-wave functions were expanded in plane waves with an energy cutoff of 400 eV. The molecule/graphene system is modeled using a supercell containing a layer of molecules adsorbed on a single layer of graphene. Test calculations showed that a vacuum layer of 12 Å are sufficient to prevent spurious interaction between systems in neighboring cells due to the periodic boundary condition. In the actual calculations, a vacuum layer of thickness 15 Å was used. Dipole moments due to asymmetric adsorption of single molecule or CTC on only one side of graphene were taken into account by the dipole correction.[37] All molecule/graphene structures were fully optimized by allowing all degrees of freedom of the systems to relax until the force acting on each atom was below 0.01 eV/Å. The tetrahedron method with Blöchl corrections[38] was used in the total energy calculations to achieve a high accuracy.

Experimentally, ultrathin epitaxial graphene (EG) samples with 1–2 layer thickness were prepared by thermal annealing of a *n*-type Si-terminated 6H-SiC(0001) sample (CREE Research Inc.) at around 1200–1300 °C in ultrahigh vacuum (UHV).[39–41] The structure of EG was confirmed by *in situ* low-energy electron diffraction, scanning tunneling microscopy, angle-resolved photoemission spectroscopy, and Raman spectroscopy.[39–41] The PES experiment was carried out at the surface, interface, and nanostructure science beamline and end station of the Singapore Synchrotron Light Source.[24] F4-TCNQ and TCNQ molecules (Sigma-Aldrich) were evaporated *in situ* from a low-temperature Knudsen cell (MBE-Komponenten, Germany) onto EG at RT in the main UHV chamber. The nominal thickness of F4-TCNQ and TCNQ was estimated by monitoring the attenuation in intensity of the Si 2*p* peak of bulk SiC before and after deposition.[42] The experiment was performed with sequential deposition/measurement stages.

III. RESULTS AND DISCUSSION

We first studied adsorption of single molecules on graphene. Figure 1(a) shows the optimized structures of the molecules being considered adsorbed on graphene. Three adsorption sites, with the center of the molecule atop a carbon atom (*t*), at the bridge site (*b*), and the hollow site (*h*), respectively, as indicated in Fig. 1(a), were considered for each molecule. At each adsorption site, different orientations of the molecule were also considered. Only the most stable configuration is shown in Fig. 1(a) for each molecule. The adsorption energies, calculated from $E_{ad}=-(E_{mol/g}-E_g-E_{mol})$, where $E_{mol/g}$, E_g, and E_{mol} are the total energy of the adsorbed system, the total energy of graphene, and the total energy of a single molecule, respectively, are 1.28, 1.15, and 0.72 eV for F4-TCNQ, TCNQ, and TTF on graphene, respectively. This indicates that F4-TCNQ has the strongest interaction while TTF has the weakest interaction with graphene. The calculated adsorption energies are expected to be slightly overestimated due to the LDA exchange-correlation functional. When TTF molecule is adsorbed on graphene, the flat molecule becomes slightly bent with atoms at the ends of the molecule being 0.4 Å closer to the graphene plane than atoms in the middle of the molecule. TCNQ and F4-TCNQ molecules are also bent when adsorbed on graphene but to a lesser degree. Heights of atoms in the TCNQ and F4-TCNQ molecules above the graphene plane differ by no more than 0.2 Å. Structures of CTCs can be very complicated and dependent on the types and relative amounts of different molecules. In this study, we consider two CTCs, i.e., TTF/TCNQ and TTF/F4-TCNQ, each with a 1:1 ratio of TTF and TCNQ or F4-TCNQ. Their optimum adsorption geometry is shown in Fig. 1(b). Compare to single-molecule TTF adsorbed on graphene, TTF in the CTCs is slightly higher above the graphene plane and the molecule is also stretched along its long axis. This is attributed to the intermolecular hydrogen-bonding network between nitrogen and hydrogen as marked by pink lines in Fig. 1(b). In contrast, there is little structural deformation in TCNQ or F4-TCNQ in CTCs compared to single molecules on graphene.

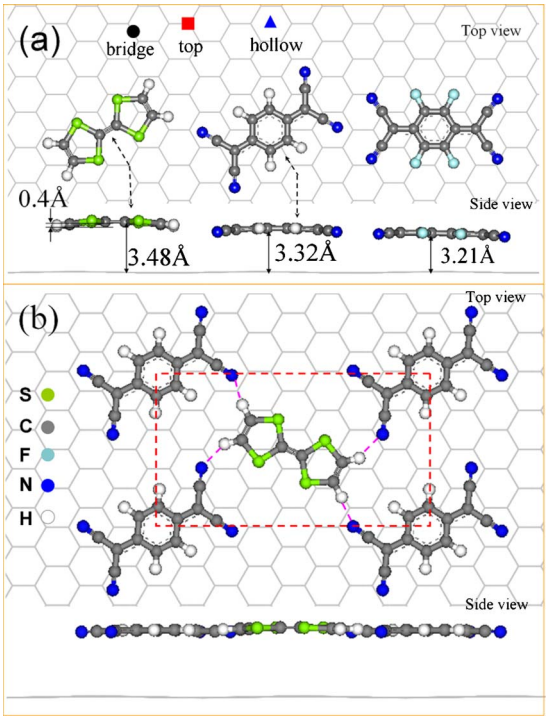

FIG. 1. (Color online) (a) The most stable configurations of single molecule on graphene. The black circle, red square, and blue triangle symbols indicate possible adsorption sites. (b) The top view and side view of the proposed model of CTC adsorbed on graphene. Red dashed lines indicate the supercell used in DFT the calculation.

To investigate the doping behavior of graphene, we calculated the differential charge density (DCD) of the adsorbed configurations

$$\Delta\rho_{mol/g} = \rho_{mol/g} - \rho_{mol} - \rho_g, \quad (1)$$

where $\rho_{mol/g}$, ρ_{mol}, and ρ_g are the charge density of the adsorbed system, the charge density of molecule, and the charge density of graphene. ρ_{mol} and ρ_g are obtained using

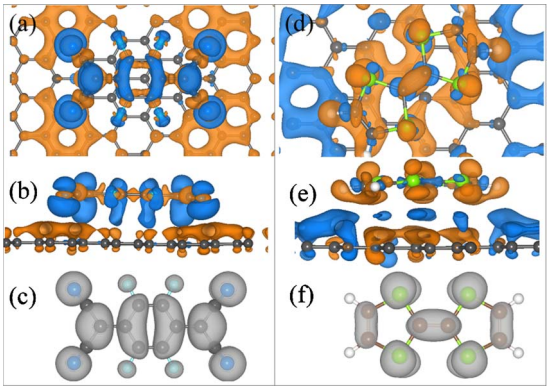

FIG. 2. (Color online) The top view [(a) and (d)] and side view [(b) and (e)] of the charge rearrangement of F4-TCNQ (left) and TTF (right) on graphene. (c) and (f) show the differential charge density isosurface of F4-TCNQ and TTF adsorbed on graphene around the Fermi level, respectively. Blue (orange) color indicates charge accumulation (depletion) region.

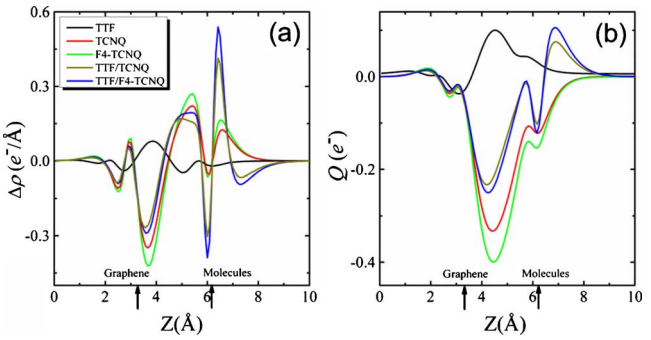

FIG. 3. (Color online) (a) Planar averaged DCD, $\Delta\rho$, induced by single molecule and CTC adsorption on graphene. Positive (negative) value corresponds to the electron accumulation (depletion). (b) The integrated DCD up to a plane at z along the normal direction of the graphene plane. The positions of graphene and adsorbate are indicated by the arrows.

the structures optimized when the molecule is adsorbed on graphene. The calculated DCD of F4-TCNQ is shown in Figs. 2(a)–2(c), which reveal nonuniform interaction behavior between F4-TCNQ and graphene. Charge transfer can be observed from graphene (orange color) to the molecule (blue color) which results in p doping of graphene. The charge transfer also alters the charge distributions around the central benzene ring and the cyano functional group of the F4-TCNQ molecule. This means that F4-TCNQ interacts strongly with graphene. The differential charge density of F4-TCNQ adsorbed on graphene and the lowest unoccupied molecular orbital (LUMO) of isolated F4-TCNQ are found similar, which indicates that charge is transferred from graphene to the LUMO of F4-TCNQ. Furthermore, charge depletion is also observed in the molecular plane, or its σ orbitals, which may be due to the back donation of the deep-lying molecular orbitals of F4-TCNQ to graphene.[43] Back donation in this system is interesting because molecules can donate electrons to the graphene substrate without bending the molecular skeletons, unlike the case of F4-TCNQ on metal surface.[43,44] The π orbitals are strongly polarized by the interaction between F4-TCNQ and graphene. The charge-transfer features of TCNQ molecule are very similar to that of F4-TCNQ because of their similar molecular structures, except that the amount of charge transferred from graphene to TCNQ is smaller than that between F4-TCNQ and graphene, which indicates that the interaction between TCNQ and graphene is weaker than that between F4-TCNQ and graphene.[24]

Upon adsorption of the donor molecule TTF on graphene, charge is transferred from the π orbital-dominated highest occupied molecular orbital of TTF to the π orbitals of graphene, as shown in Figs. 2(d)–2(f). In contrast to the case of F4-TCNQ and TCNQ on graphene, the amount of charge transfer is much smaller and the charges accumulate on the σ orbitals of TTF. The most important feature upon adsorption of TTF on graphene is that there is a screening layer at the interface, which prevents further charge transfer from TTF to graphene. Charge transfers between the CTCs and graphene, when CTCs are adsorbed on graphene, are similar to that between the respective single molecules and graphene, despite the TTF has a larger separation from the graphene plane.

It is not easy to quantify accurately the charge transfer between an adsorbate and the substrate from plane-wave DFT calculations as charges on the adsorbate and substrate cannot be distinguished due to the delocalized electron-wave functions. Nevertheless, planar averaged DCD may provide some useful information on the bonding mechanism and charge redistribution. To do this, the DCD is integrated over the x-y plane (graphene plane)[45]

$$\Delta\rho_{\mathrm{mol/g}}(z) = \int \Delta\rho_{\mathrm{mol/g}}(x,y,z)dxdy. \tag{2}$$

The calculated planar averaged DCDs are shown in Fig. 3(a) as a function of z (normal to the graphene plane), where the two arrows indicate positions of graphene and adsorbed molecule. Two kinds of doping behaviors, i.e., p and n doping, on graphene are clearly distinguishable. It is clear that charges are accumulated on the molecule side in the cases of F4-TCNQ and CTC on graphene but TTF molecule donates electrons to graphene. This is determined by the molecular intrinsic properties. TTF, TCNQ/F4-TCNQ molecules have smaller and larger ionization potentials, respectively, than graphene.[43,46] This is in contrast to the case of TCNQ on Au(111), where TCNQ weakly interacts with the herringbone substrate.[28,47] The fact that F4-TCNQ molecules attract electrons from graphene is also in agreement with the results of recent experiment.[24] We can expect the dipole moment at the interface between TTF and graphene to be opposite to that of TCNQ or F4-TCNQ on graphene, and the dipole moment between TCNQ or F4-TCNQ and graphene to be larger than that of TTF on graphene, due to the amounts of charge transfer and resulting Coulomb interaction between the molecules and graphene. This is in qualitative agreement with the calculated adsorption energies.

The total amount of charge transfer crossing a plane parallel to the graphene layer can be estimated by simply inte-

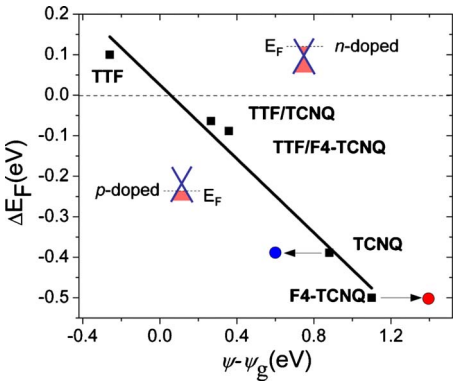

FIG. 4. (Color online) The Fermi level variation (ΔE_F, relative to the Dirac point) as a function of the potential step. The black line is the linear fit to the theoretical data points (square). Red circles indicate the experimental PES data.

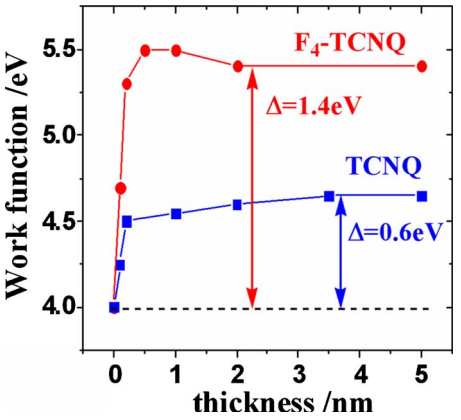

FIG. 5. (Color online) Work function of epitaxially grown graphene on silicon carbide as a function of the molecular coverage. Red and blue symbols correspond to F4-TCNQ and TCNQ doping, respectively.

grating the planar averaged DCD $\Delta\rho_{\mathrm{mol/g}}$ up to the plane (at height z)[43]

$$Q(z) = \int_0^z \Delta\rho_{\mathrm{mol/g}}(z')dz'. \tag{3}$$

As shown in Fig. 3(b), the charge transfer reaches a maximum at about 1.5 Å above the graphene plane for F4-TCNQ adsorbed on graphene and the amount of charge transferred from graphene to the molecule is about $0.4e$. In other cases, roughly $0.33e$, $0.25e$, and $0.23e$ are transferred from graphene to TCNQ, TTF/F4-TCNQ CTC, and TTF/TCNQ CTC, respectively, while each TTF molecule donates about $0.1e$ to graphene. In addition, the charge analysis is conducted by Bader scheme, which give an intuitive way of dividing charge into each atom for plane-wave-based DFT calculations.[48–50] The estimated values of charge transfer for TTF, TCNQ, F4-TCNQ, TTF/TCNQ, and TTF/F4-TCNQ on graphene are $0.07e$, $0.34e$, $0.44e$, $0.19e$, and $0.24e$, respectively, which are in good agreement with that estimated by Eq. (3).

The band structure of graphene has a linear energy-dispersion relationship around the Dirac point where the conduction band and valence band touch at K points in the first Brillouin Zone. The position of the Fermi level relative to the Dirac point is directly related to the type and concentration of charge carrier in graphene. Figure 4 shows the calculated relative position between the Fermi level and the Dirac point, ΔE_F, as a function of change in work function of graphene upon molecular adsorption ψ-ψ_g, where ψ_g (4.54 eV) and ψ are the work functions of graphene before and after molecular adsorption. It is clear that the Fermi level of TTF-adsorbed graphene is above the Dirac point, indicating charge transfer from the donor molecule to graphene, and n-type doping of graphene. The Fermi levels of all other systems being considered are below the Dirac point of graphene, confirming charge transfer from graphene to the molecules and p doping of graphene. These results are in agreement with above charge-transfer analysis.

The adsorbate induced change in work function of graphene, with respect to that of pristine graphene, is referred as a potential step $\Delta\psi$. As shown in Fig. 4, TTF on graphene has a negative potential step. In contrast, F4-TCNQ adsorbed graphene has a positive potential step, followed by TCNQ adsorbed graphene, due to strong molecule-graphene interaction. In order to verify this trend in potential step, we carried out *in situ* PES experiments. Vacuum-level shift was determined from PES spectra at the low kinetic-energy onset (secondary electron cutoff) using photon energy of 60 eV with −5 V sample bias. Sample work functions (ψ) were obtained through the equation, $\psi = h\upsilon - W$, where W is the spectrum width (the energy difference between the substrate Fermi level and low kinetic-energy onset).[51] As shown in Fig. 5, the work functions of TCNQ or F4-TCNQ modified graphene samples increase linearly with the increasing coverage of molecules at the initial state and finally approaches a constant at higher coverage. The measured increases in work functions at higher coverage upon the molecular adsorption are about 0.6 and 1.4 eV for TCNQ and F4-TCNQ modified graphene samples, respectively. These two values agree well with the theoretical potential step, 0.88 and 1.1 eV for TCNQ and F4-TCNQ on graphene, respectively. Furthermore, the change in work function for F4-TCNQ modified graphene sample is larger than that for TCNQ modified graphene samples, in good agreement with the theoretical trend of work function (Fig. 5).

The change in potential step of these investigated systems are due to the interfacial dipole created by charge transfer between molecules and graphene.[52] In the case of F4-TCNQ on graphene the charge transfer from graphene to F4-TCNQ on graphene causes a negative dipole pointing toward graphene. In contrast, the charge transfer in reverse direction in the case of TTF on graphene creates a positive dipole pointing toward TTF molecule. One can expect the work function of TTF-adsorbed graphene will decrease due to the positive dipole and increase for F4-TCNQ on graphene. For the CTC systems, the change in work functions is more complex, and depends on the relative ratio of molecules with different electron affinities. For the TTF and F4-TCNQ CTC considered here, a 1:1 ratio is assumed. TTF and F4-TCNQ create positive and negative dipoles at the interface, respec-

tively. Since F4-TCNQ has a larger negative dipole, the work function of TTF and F4-TCNQ on graphene is dominated by F4-TCNQ, leading to a net negative dipole. Another case of CTC (TTF and TCNQ) on graphene is very similar except that the interface dipole is smaller.

This linear dependence of Fermi level on the potential step shown in Fig. 4 suggests that the interaction between single molecule and graphene is dominated by the charge transfer between graphene and the adsorbed molecules. This linear relationship is obeyed more strictly by single molecule on graphene and a slight deviation from the linear fit is observed for CTCs on graphene. It is reported that the chemical interaction can lead to nonlinear contributions to the bonding behavior.[9] The slight deviation from the linear behavior of CTCs on graphene may be due to the intermolecular hydrogen-bonding network. The differential charge density of CTCs on graphene shows that the intermolecular interaction is dominated by the antibonding state between them, which demonstrates that the intermolecular charge transfer is indirectly through the graphene surface.

The CTCs on graphene may give rise to a mixed phase with tunable electronic properties. As discussed above, the acceptor molecules (TCNQ and F4-TCNQ) have stronger interactions with graphene than the donor molecule (TTF). This interfacial interaction is different from that of CTCs on metal substrate such as Au(111), where the donor molecule has strong interactions with the metal surface and the gold substrate is almost unperturbed by the acceptor molecules.[28] This is ascribed to the formation of a quasi-one-dimensional electronic-band dispersion and the anisotropic structure of the molecular layer. In contrast, the strong interaction between acceptor molecules and graphene induces a band-gap opening in graphene which is 0.198 eV for F4-TCNQ adsorbed graphene and 0.175 eV for TCNQ adsorbed graphene, respectively. This is because the strong interaction between acceptor molecules and graphene breaks the sixfold symmetry of graphene. These features of single molecule and CTC on graphene are important and deserve further experimental investigations. The linear doping behavior of graphene by organic molecules may provide a possible way to control the type and concentration of charge carrier in graphene and to tune the electrical properties of graphene.

IV. CONCLUSIONS

First-principles calculations and photoemission spectroscopy experiments were carried out to investigate the electronic properties of graphene doped by a number of organic molecules and their CTCs. It is found that graphene can be made *n* or *p* type by doping with strong donor or acceptor molecules, respectively. Theoretical predictions based on DFT calculations are in good agreement with experimental results. More importantly, the type and concentration of charge carrier in graphene can be tuned continuously and linearly by CTCs consisting of different molecules. Interaction between the adsorbates and graphene is dominated by a charge-transfer mechanism. Results of the present work suggest that the electronic structure of graphene can be engineered by suitable composition of CTC.

ACKNOWLEDGMENTS

This research is supported by Singapore NRF under Grant No. R-143-000-360-281 "Graphene Related Materials and Devices" and Singapore ARF under Grant No. R-143-000-392-133.

*phyfyp@nus.edu.sg
†phyweets@nus.edu.sg

[1] K. S. Novoselov, A. K. Geim, S. V. Morozov, D. Jiang, Y. Zhang, S. V. Dubonos, I. V. Grigorieva, and A. A. Firsov, Science **306**, 666 (2004).
[2] K. S. Novoselov, D. Jiang, F. Schedin, T. J. Booth, V. V. Khotkevich, S. V. Morozov, and A. K. Geim, Proc. Natl. Acad. Sci. U.S.A. **102**, 10451 (2005).
[3] K. S. Novoselov, A. K. Geim, S. V. Morozov, D. Jiang, M. I. Katsnelson, I. V. Grigorieva, S. V. Dubonos, and A. A. Firsov, Nature (London) **438**, 197 (2005).
[4] A. H. Castro Neto, F. Guinea, N. M. R. Peres, K. S. Novoselov, and A. K. Geim, Rev. Mod. Phys. **81**, 109 (2009).
[5] T. O. Wehling, I. Grigorenko, A. I. Lichtenstein, and A. V. Balatsky, Phys. Rev. Lett. **101**, 216803 (2008).
[6] Y. B. Zhang, T.-T. Tang, C. Girit, Z. Hao, M. C. Martin, A. Zettl, M. F. Crommie, Y. R. Shen, and F. Wang, Nature (London) **459**, 820 (2009).
[7] K. S. Novoselov, E. McCann, S. V. Morozov, V. I. Fal'ko, M. I. Katsnelson, U. Zeitler, D. Jiang, F. Schedin, and A. K. Geim, Nat. Phys. **2**, 177 (2006).
[8] S. Y. Zhou, D. A. Siegel, A. V. Fedorov, and A. Lanzara, Phys. Rev. Lett. **101**, 086402 (2008).
[9] S. K. Saha, R. Ch. Chandrakanth, H. R. Krishnamurthy, and U. V. Waghmare, Phys. Rev. B **80**, 155414 (2009).
[10] D. C. Elias, R. R. Nair, T. M. G. Mohiuddin, S. V. Morozov, P. Blake, M. P. Halsall, A. C. Ferrari, D. W. Boukhvalov, M. I. Katsnelson, A. K. Geim, and K. S. Novoselov, Science **323**, 610 (2009).
[11] J. Zhou, Q. Wang, Q. Sun, X. S. Chen, Y. Kawazoe, and P. Jena, Nano Lett. **9**, 3867 (2009).
[12] A. K. Singh and B. I. Yakobson, Nano Lett. **9**, 1540 (2009).
[13] F. Guinea, M. I. Katsnelson, and A. K. Geim, Nat. Phys. **6**, 30 (2009).
[14] S. M. Choi and S. H. Jhia, Appl. Phys. Lett. **94**, 153108 (2009).
[15] C. H. Park, L. Yang, Y. W. Son, M. L. Cohen, and S. G. Louie, Nat. Phys. **4**, 213 (2008).
[16] C. H. Park, L. Yang, Y. W. Son, M. L. Cohen, and S. G. Louie, Phys. Rev. Lett. **101**, 126804 (2008).
[17] T. Ohta, A. Bostwick, T. Seyller, K. Horn, and E. Rotenberg, Science **313**, 951 (2006).
[18] T. O. Wehling, K. S. Novoselov, S. V. Morozov, E. E. Vdovin, M. I. Katsnelson, A. K. Geim, and A. I. Lichtenstein, Nano Lett. **8**, 173 (2008).
[19] Y. H. Lu, W. Chen, Y. P. Feng, and P. M. He, J. Phys. Chem. B **113**, 2 (2009).

[20] G. Giovannetti, P. A. Khomyakov, G. Brocks, V. M. Karpan, J. van den Brink, and P. J. Kelly, Phys. Rev. Lett. **101**, 026803 (2008).
[21] Y. Pan, H. G. Zhang, D. X. Shi, J. T. Sun, S. X. Du, F. Liu, and H.-J. Gao, Adv. Mater. **21**, 2777 (2009).
[22] P. A. Khomyakov, G. Giovannetti, P. C. Rusu, G. Brocks, J. van den Brink, and P. J. Kelly, Phys. Rev. B **79**, 195425 (2009).
[23] I. Gierz, C. Riedl, U. Starke, C. R. Ast, and K. Kern, Nano Lett. **8**, 4603 (2008).
[24] W. Chen, S. Chen, Q. C. Qi, X. Y. Gao, and A. T. S. Wee, J. Am. Chem. Soc. **129**, 10418 (2007).
[25] R. Voggu, B. Das, C. S. Rout, and C. N. R. Rao, J. Phys.: Condens. Matter **20**, 472204 (2008).
[26] H. Alves, A. S. Molinari, H. Xie, and A. F. Morpurgo, Nature Mater. **7**, 574 (2008).
[27] I. Avilov, V. Geskin, and J. Cornil, Adv. Funct. Mater. **19**, 624 (2009).
[28] N. Gonzalez-Lakunza, I. Fernandez-Torrente, K. J. Franke, N. Lorente, A. Arnau, and J. I. Pascual, Phys. Rev. Lett. **100**, 156805 (2008).
[29] I. Fernández-Torrente, K. J. Franke, and J. I. Pascual, Phys. Rev. Lett. **101**, 217203 (2008).
[30] G. Kresse and J. Furthmüller, Phys. Rev. B **54**, 11169 (1996).
[31] G. Kresse and J. Hafner, Phys. Rev. B **47**, 558 (1993).
[32] G. Kresse and J. Hafner, Phys. Rev. B **49**, 14251 (1994).
[33] G. Kresse and J. Furthmüller, Comput. Mater. Sci. **6**, 15 (1996).
[34] J. P. Perdew and A. Zunger, Phys. Rev. B **23**, 5048 (1981).
[35] P. E. Blöchl, Phys. Rev. B **50**, 17953 (1994).
[36] G. Kresse and D. Joubert, Phys. Rev. B **59**, 1758 (1999).
[37] G. Makov and M. C. Payne, Phys. Rev. B **51**, 4014 (1995).
[38] P. E. Blöchl, O. Jepsen, and O. K. Andersen, Phys. Rev. B **49**, 16223 (1994).
[39] W. Chen, H. Xu, L. Liu, X. Y. Gao, D. C. Qi, G. W. Peng, S. C. Tan, Y. P. Feng, K. P. Loh, and T. S. W. Andrew, Surf. Sci. **596**, 176 (2005).
[40] H. Huang, W. Chen, S. Chen, and A. T. S. Wee, ACS Nano **2**, 2513 (2008).
[41] Z. H. Ni, W. Chen, X. F. Fan, J. L. Kuo, T. Yu, A. T. S. Wee, and Z. X. Shen, Phys. Rev. B **77**, 115416 (2008).
[42] M. P. Seah and W. A. Dench, Surf. Interface Anal. **1**, 2 (1979).
[43] G. M. Rangger, O. T. Hofmann, L. Romaner, G. Heimel, B. Broker, R. P. Blum, R. L. Johnson, N. Koch, and E. Zojer, Phys. Rev. B **79**, 165306 (2009).
[44] L. Romaner, G. Heimel, J.-L. Brédas, A. Gerlach, F. Schreiber, R. L. Johnson, J. Zegenhagen, S. Duhm, N. Koch, and E. Zojer, Phys. Rev. Lett. **99**, 256801 (2007).
[45] A. Michaelides, P. Hu, M. H. Lee, A. Alavi, and D. A. King, Phys. Rev. Lett. **90**, 246103 (2003).
[46] K. F. Braun and S. W. Hla, J. Chem. Phys. **129**, 064707 (2008).
[47] I. F. Torrente, K. J. Franke, and J. I. Pascual, Int. J. Mass Spectrom. **277**, 269 (2008).
[48] G. Henkelman, A. Arnaldsson, and H. Jónsson, Comput. Mater. Sci. **36**, 354 (2006).
[49] E. Sanville, S. D. Kenny, R. Smith, and G. Henkelman, J. Comput. Chem. **28**, 899 (2007).
[50] W. Tang, E. Sanville, and G. Henkelman, J. Phys.: Condens. Matter **21**, 084204 (2009).
[51] H. Ishii, K. Sugiyama, E. Ito, and K. Seki, Adv. Mater. **11**, 605 (1999).
[52] T. C. Leung, C. L. Kao, W. S. Su, Y. J. Feng, and C. T. Chan, Phys. Rev. B **68**, 195408 (2003).